JOURNAL OF SOLID STATE CHEMISTRY 44, 273–281 (1982)

Structural Chemistry of the Magnéli Phases Ti_nO_{2n-1}, $4 \leq n \leq 9$

II. Refinements and Structural Discussion

Y. LE PAGE AND PIERRE STROBEL

Solid State Chemistry, National Research Council of Canada, Ottawa K1A 0R9, Canada

Received March 10, 1982; in final form April 30, 1982

The structures of the title compounds $6 \leq n < 9$ were refined from single-crystal X-ray diffraction intensities. The pattern of edge- and corner-sharing between TiO_6 octahedra permits description of the structures by means of strongly bonded (101) layers containing two directions of chains: a $[\bar{1}01]$ chain with rutile-like chain segments and a [010] chain in the shear-plane region. These layers are joined by corner-sharing only. The structures can also be described as the alternate stacking of a fixed-geometry shear-region slab four octahedra thick and a rutile-like slab $(n - 4)$ octahedra thick in which edge-sharing occurs only inside the pseudorutile chain segments. The family is remarkably homogeneous with similar ionic valences and similar distortions of the Ti–O and Ti–Ti distances for corresponding atoms in different members. As noted before for cell parameters, Ti_4O_7 is slightly different from the others probably due to the absence of a rutile-like slab. No even–odd alternance was noted.

Introduction

The compounds Ti_nO_{2n-1} have raised considerable interest, both because of their surprising building principle and of their unusual electrical properties, large discontinuities in the electrical conductivity being observed at phase transitions which occur at low temperature. The compounds with $4 \leq n \leq 9$ were prepared in powder form by Andersson and co-workers (*1*, *2*), who proposed a theoretical model for cell parameters and atomic structures in this series. Compounds with larger values of n were studied by Bursill and Hyde (*3*) with use of electron diffraction and high-resolution microscopy. The members Ti_4O_7 and Ti_5O_9 have been prepared in single-crystal form (*4*) and their structures and physical properties have been thoroughly studied by Marezio *et al.* (*5*, *6*) both at room and low temperatures. Single crystals of Ti_6O_{11}, Ti_7O_{13}, Ti_8O_{15}, and Ti_9O_{17} were prepared by chemical vapor transport (*7*, *8*) for a study of their physical properties. As no single-crystal structural results were available, a structural study was undertaken for comparison with the model structures (*9*) and to observe the evolution of the pattern of valences for Ti atoms at room temperature throughout the series.

Experimental

The diffraction intensities of a broken piece of a single crystal of Ti_9O_{17} with faces approximately 0.3 mm in all dimensions were measured at 25°C. Graphite-monochromatized Mo$K\alpha$ radiation generated at 50 kV, 10 mA was used in a $\theta/2\theta$ scan with line-profile analysis. A total of 8101 measurements were made up to 80° 2θ giving 6811 valid unique reflections of which 5507 had a net intensity larger than three count-

0022-4596/82/110273-09$02.00/0

TABLE I

DETAILS OF THE VARIOUS DATA COLLECTIONS

Compound	Ti_6O_{11}	Ti_7O_{13}	Ti_8O_{15}	Ti_9O_{17}
Space group	$I\bar{1}$	$I\bar{1}$	$I\bar{1}$	$I\bar{1}$
a (Å)	5.552(1)	5.537(1)	5.526(1)	5.524(1)
b (Å)	7.126(1)	7.132(1)	7.133(1)	7.142(1)
c (Å)	32.233(6)	38.151(8)	44.059(6)	50.03(1)
α	66.94(1)	66.70(1)	66.54(1)	66.41(1)
β	57.08(1)	57.12(1)	57.18(1)	57.20(1)
γ (deg)	108.51(2)	108.50(2)	108.51(1)	108.53(1)
Maximum 2θ ($MoK\alpha_1$) (deg)	90	80	80	80
Unique measurements	5922	5237	5993	6811
Observed (3 sigmas)	4094	3007	3982	5507
R_{sym}	0.030	No mult. meas.	No mult. meas.	0.020
Largest dimension of sample (mm)	0.30	0.15	0.20	0.30
Shape of sample	Broken with faces	Equidimens. chunk	Equidimens. chunk	Broken with faces
Absorption correction	Gaussian	Spherical	Spherical	Gaussian
Final residuals				
R_F	0.039[a]	0.036	0.030	0.025
wR_F	0.045	0.041	0.031	0.026

[a] This sample showed a very severe case of extinction.

ing statistics sigmas and were considered to be observed. The mean deviation of the equivalent intensities with respect to their average was 2.0%. The intensities were corrected for measured direct beam polarization (0.970). A Gaussian absorption correction was performed ($\mu = 62.7\ cm^{-1}$). The cell parameters were obtained by least-squares refinement of the setting angles of 56 reflections with 2θ values larger than 60° ($\lambda MoK\alpha_1 = 0.70932$ Å). The periods along **a**, **b**, and [111] were checked by means of oscillation pictures. The model (*2*) reformulated to use a cell based on the mesh in the shear plane and the period along the pseudorutile direction (*9*) was used as a starting point for the refinement. The atoms were refined anisotropically by block-diagonal least-squares using counting statistics weights. An extinction correction was included (*10*). The scattering curves for neutral atoms were taken from (*11*). The final residuals were $R_F = 0.025$ and $wR_F = 0.026$.

The studies of the other three compounds follow quite closely the above experimental technique. The numerical details of the various data collections are summarized in Table I and the final atomic parameters are in Table II.[1]

Description of the Structures

The previous description (*2*) based on the interpretation of the X-ray powder patterns is essentially correct. A few points which were not clearly stated in previous descriptions follow. Figure 1 is an orthogonal projection of a slab parallel to the **a c** plane with $-0.3 < y < 0.3$ onto a plane approximately perpendicular to **b** for Ti_6O_{11}. It shows the

[1] Structure factor tables and anisotropic thermal motion tables are deposited with ASIS/NAPS, document number NAPS-03965 (150 pages).

TABLE IIa

ATOMIC PARAMETERS X, Y, Z, AND Beq FOR Ti_8O_{11}

	X	Y	Z	Beq
Ti(1,1)	0.01694(18)	0.01249(13)	0.04189(3)	0.43(4)
Ti(1,2)	0.04804(17)	0.04599(12)	0.12796(3)	0.42(4)
Ti(1,3)	0.08925(17)	0.03991(12)	0.21912(3)	0.39(4)
Ti(2,1)	0.01538(19)	0.51222(13)	0.04304(3)	0.51(4)
Ti(2,2)	0.04278(17)	0.53903(12)	0.12984(3)	0.41(4)
Ti(2,3)	0.09235(17)	0.54489(12)	0.21673(3)	0.38(4)
O(1,1)	−0.0195(7)	0.6931(5)	0.07571(12)	0.51(18)
O(1,2)	−0.0770(7)	0.6704(5)	0.17792(11)	0.45(17)
O(2,0)	0.0336(7)	0.3219(5)	0.01279(12)	0.49(17)
O(2,1)	0.0583(7)	0.3383(5)	0.10073(12)	0.51(18)
O(2,2)	0.0325(7)	0.3150(5)	0.19623(11)	0.44(17)
O(3,1)	0.6036(7)	0.8195(5)	0.05449(12)	0.57(17)
O(3,2)	0.6344(7)	0.8401(5)	0.14142(12)	0.55(18)
O(3,3)	0.6231(7)	0.8426(5)	0.23277(11)	0.43(16)
O(4,0)	0.4055(7)	0.1862(5)	0.03826(11)	0.52(17)
O(4,1)	0.4127(7)	0.1885(5)	0.12846(11)	0.47(16)
O(4,2)	0.4436(7)	0.1793(5)	0.21666(11)	0.45(17)

Note. Beq is the arithmetic mean of the principal axes of the thermal ellipsoid. ESDs refer to the last digit. The nomenclature follows (9).

pseudorutile chain segments parallel to the z axis and extending from $z = \frac{1}{4}$ to $\frac{3}{4}$ made of six edge-sharing TiO_6 octahedra. These segments link by face-sharing of the terminal

TABLE IIb

ATOMIC PARAMETERS X, Y, Z, AND Beq FOR Ti_7O_{13}

	X	Y	Z	Beq
Ti(1,0)	0	0	0	0.49(9)
Ti(1,1)	0.02289(24)	0.01798(17)	0.07288(3)	0.45(6)
ti(1,2)	0.05373(23)	0.05037(16)	0.14620(3)	0.45(6)
Ti(1,3)	0.09013(23)	0.04081(16)	0.22389(3)	0.41(6)
Ti(2,0)	0	½	0	0.51(9)
Ti(2,1)	0.02534(24)	0.51812(17)	0.07388(4)	0.54(6)
ti(2,2)	0.04851(23)	0.54356(16)	0.14797(3)	0.42(6)
Ti(2,3)	0.09374(23)	0.54566(16)	0.22168(3)	0.40(6)
O(1,0)	−0.0163(9)	0.6883(6)	0.02573(13)	0.5(3)
O(1,1)	−0.0101(9)	0.6993(6)	0.10149(14)	0.5(3)
O(1,2)	−0.0736(9)	0.6742(6)	0.18849(13)	0.47(25)
O(2,0)	0.0306(9)	0.3227(6)	0.04987(13)	0.5(3)
O(2,1)	0.0594(9)	0.3402(6)	0.12404(13)	0.5(3)
O(2,2)	0.0336(9)	0.3155(6)	0.20471(13)	0.42(25)
O(3,0)	0.6002(9)	0.8098(6)	0.00662(13)	0.52(24)
O(3,1)	0.6147(9)	0.8255(6)	0.08371(14)	0.53(25)
O(3,2)	0.6411(9)	0.8441(6)	0.15710(13)	0.51(24)
O(3,3)	0.6219(9)	0.8418(6)	0.23535(13)	0.43(24)
O(4,0)	0.4061(9)	0.1927(6)	0.07037(13)	0.51(24)
O(4,1)	0.4158(9)	0.1926(6)	0.14683(13)	0.47(25)
O(4,2)	0.4448(9)	0.1816(6)	0.22180(13)	0.5(3)

Note. Beq is the arithmetic mean of the principal axes of the thermal ellipsoid. ESDs refer to the last digit. The nomenclature follows (9).

TABLE IIc

ATOMIC PARAMETERS X, Y, Z, AND Beq FOR Ti_8O_{15}

	X	Y	Z	Beq
Ti(1,1)	0.00490(17)	0.00533(12)	0.032342(21)	0.49(3)
Ti(1,2)	0.03156(16)	0.02307(11)	0.095798(19)	0.45(4)
Ti(1,3)	0.05726(15)	0.05485(10)	0.159757(19)	0.41(4)
Ti(1,4)	0.09216(15)	0.04119(10)	0.227222(19)	0.40(4)
Ti(2,1)	0.01200(17)	0.50575(12)	0.032364(21)	0.50(4)
Ti(2,2)	0.03377(16)	0.52580(11)	0.096572(20)	0.50(4)
Ti(2,3)	0.05330(15)	0.54622(10)	0.161410(19)	0.41(4)
Ti(2,4)	0.09541(15)	0.54753(10)	0.225196(19)	0.40(4)
O(1,1)	0.9921(6)	0.6946(4)	0.05492(8)	0.48(17)
O(1,2)	0.9960(6)	0.7047(4)	0.12063(8)	0.51(16)
O(1,3)	0.9271(6)	0.6759(4)	0.19678(8)	0.48(16)
O(2,0)	0.0128(6)	0.3120(4)	0.01151(8)	0.46(16)
O(2,1)	0.0328(6)	0.3263(4)	0.07661(8)	0.46(16)
O(2,2)	0.0627(6)	0.3430(4)	0.14043(8)	0.48(16)
O(2,3)	0.0346(6)	0.3147(4)	0.21074(8)	0.44(16)
O(3,1)	0.6108(6)	0.8155(4)	0.03858(8)	0.52(17)
O(3,2)	0.6231(6)	0.8305(4)	0.10511(8)	0.53(16)
O(3,3)	0.6430(6)	0.8459(4)	0.16930(8)	0.50(16)
O(3,4)	0.6215(6)	0.8429(4)	0.23719(8)	0.47(17)
O(4,0)	0.4016(6)	0.1970(4)	0.02702(8)	0.48(16)
O(4,1)	0.4108(6)	0.1977(4)	0.09383(8)	0.47(17)
O(4,2)	0.4199(6)	0.1960(4)	0.16018(8)	0.48(16)
O(4,3)	0.4458(6)	0.1826(4)	0.22525(8)	0.45(17)

Note. Beq is the arithmetic mean of the principal axes of the thermal ellipsoid. ESDs refer to the last digit. The nomenclature follows (9).

TABLE IId

ATOMIC PARAMETERS X, Y, Z, AND Beq FOR Ti_9O_{17}

	X	Y	Z	Beq
Ti(1,0)	0	0	0	0.55(3)
Ti(1,1)	0.01284(8)	0.01106(6)	0.057343(9)	0.508(21)
Ti(1,2)	0.03725(8)	0.02811(6)	0.113554(9)	0.477(21)
Ti(1,3)	0.06027(8)	0.05701(6)	0.170154(9)	0.421(20)
Ti(1,4)	0.09266(8)	0.04166(6)	0.229844(9)	0.405(20)
Ti(2,0)	0	½	0	0.52(3)
Ti(2,1)	0.02191(8)	0.51380(6)	0.057078(9)	0.521(22)
Ti(2,2)	0.03915(8)	0.52960(6)	0.114287(9)	0.508(21)
Ti(2,3)	0.05638(8)	0.54882(6)	0.171596(9)	0.418(21)
Ti(2,4)	0.09580(8)	0.54775(6)	0.228114(9)	0.404(20)
O(1,0)	0.9956(3)	0.69378(24)	0.01865(3)	0.47(9)
O(1,1)	0.9996(3)	0.70035(24)	0.07726(4)	0.47(9)
O(1,2)	0.0026(3)	0.70937(25)	0.13528(4)	0.51(9)
O(1,3)	0.9292(3)	0.67779(25)	0.20287(4)	0.51(9)
O(2,0)	0.0144(3)	0.31481(24)	0.03964(3)	0.46(9)
O(2,1)	0.0369(3)	0.33014(24)	0.09674(3)	0.46(9)
O(2,2)	0.0655(3)	0.34573(24)	0.15317(4)	0.48(9)
O(2,3)	0.0366(3)	0.31665(24)	0.21516(3)	0.43(9)
O(3,0)	0.6069(3)	0.80771(24)	0.00511(3)	0.49(9)
O(3,1)	0.6180(3)	0.81943(25)	0.06302(3)	0.49(9)
O(3,2)	0.6283(3)	0.83343(25)	0.12169(4)	0.53(9)
O(3,3)	0.6456(3)	0.84786(25)	0.17851(4)	0.51(9)
O(3,4)	0.6226(3)	0.84322(24)	0.23860(3)	0.47(9)
O(4,0)	0.4057(3)	0.20318(25)	0.05274(3)	0.50(9)
O(4,1)	0.4148(3)	0.20198(25)	0.11185(3)	0.48(9)
O(4,2)	0.4225(3)	0.19848(24)	0.17058(3)	0.47(9)
O(4,3)	0.4479(3)	0.18366(25)	0.22803(3)	0.46(9)

Note. Beq is the arithmetic mean of the principal axes of the thermal ellipsoid. ESDs refer to the last digit. The nomenclature follows (9).

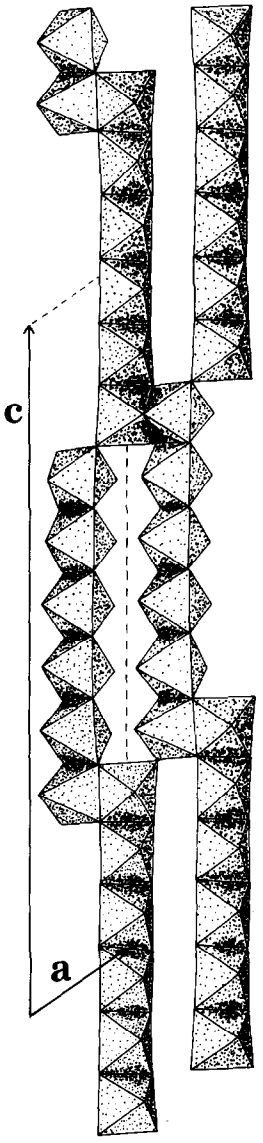

FIG. 1. Orthogonal projection of a slab $-0.3 \leq y \leq 0.3$ onto a plane approximately perpendicular to **b** for Ti_6O_{11}. The chain segments parallel to **c** and the infinite [$\bar{1}$01] chains involving face-sharing can be seen.

octahedra. Thus the direction of the infinite chains involving face-sharing is actually [$\bar{1}$01]. Figure 2 is an orthogonal projection along x of Ti_8O_{15}. The chain segments here are eight octahedra long. In the central part of the chain, only corners are shared with adjacent chains forming a rutile-like region four octahedra long. On the contrary, edge-sharing with neighboring chains occurs at the two terminal octahedra at each end of the chain segments in the vicinity of the shear plane. The complex architecture of the shear plane is shown in stereo in Fig. 3. The pattern of edge-sharing and face-shar-

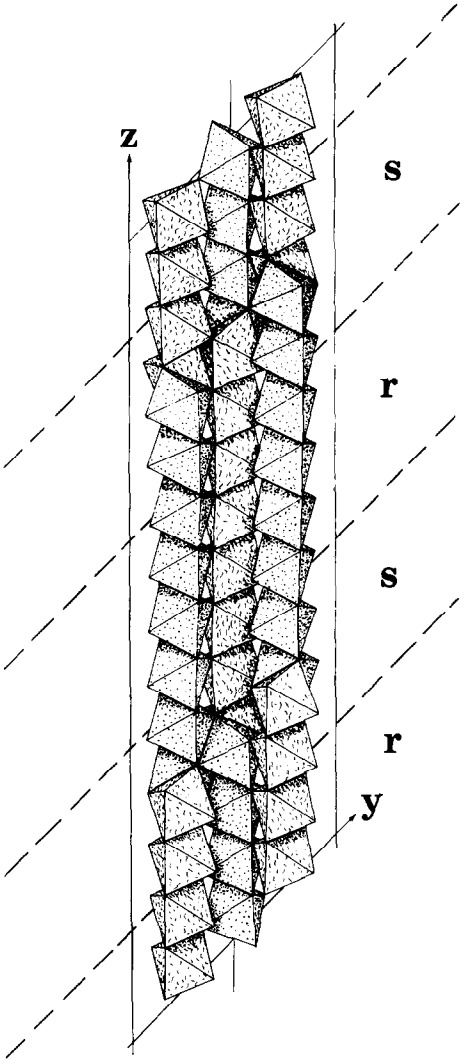

FIG. 2. Orthogonal projection along **a** for Ti_8O_{15}. The shading of the chain segments is made of dots for Ti_1 and dahses for Ti_2. The two [$\bar{1}$01] chains around the central chain correspond through an **a** + **b** translation. The rutile-like (r) and shear-plane (s) slabs are indicated.

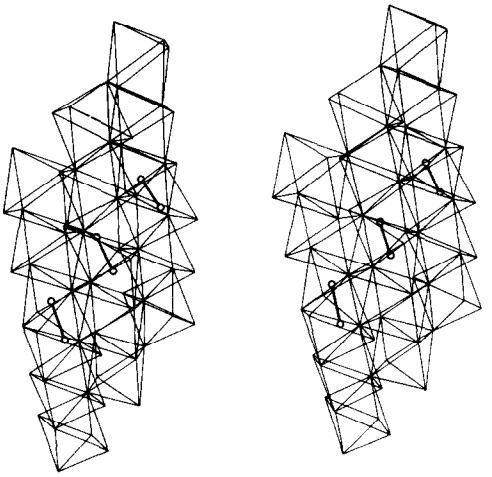

FIG. 3. Stereoscopic pair of the shear-plane region at $z = 0.25$ for Ti_8O_{15}. The orientation is similar to Fig. 2 but the two chains around the central one correspond through a **b** translation. The segments joining the Ti atoms inside the face-sharing octahedra are shown.

ing in the shear plane gives rise to strongly bonded chains parallel to **b** shown in Fig. 4. The crisscross of the **b** chains and of the [$\bar{1}$01] chains gives strongly bonded (101) layers joined to the neighboring layers by corner-sharing only.

As the members of the series differ by the length of the pseudorutile chain segments, the structures of the family can also be described as made of the stacking of alternating (001) slabs: a shear-plane slab with fixed geometry, four octahedra thick where the octahedra share three edges or one face and three edges in addition to corners and a pseudorutile slab ($n - 4$) octahedra thick where two edges and corners are shared in a rutile-like fashion.

Discussion

Valence Distribution in the Pseudorutile Chains

The above decomposition of the structure into (001) slabs is supported by the analysis of the Ti–O distances (Table III)

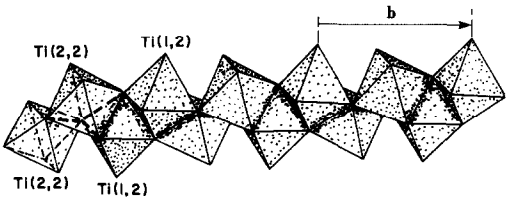

FIG. 4. The [010] chain made of the terminal TiO_6 octahedra in each chain segment is shown in the case of Ti_5O_9. Only the atom names would change for the other members of the series.

and of the corresponding ionic valences v of the Ti atoms (Table IV). These valences were derived from the average Ti–O distance $\bar{d}$ in the corresponding octahedron by interpolation between similar distances in TiO_2 and Ti_2O_3 following the analysis in (*5*). The relationship actually used was $v = 27.93 - 12.17\,\bar{d}$. The pattern of valences is remarkably consistent in the shear-plane region for $n = 6$ to 9. The corresponding valences for $n = 5$ but especially $n = 4$ turn out to be lower than for the other members of the series. We attribute this observation to the smaller average valence of Ti for small n. In the case of Ti_4O_7 the average valence is 3.5, which is less than the value of 3.6 displayed by the other members in the shear-plane region. It is therefore not

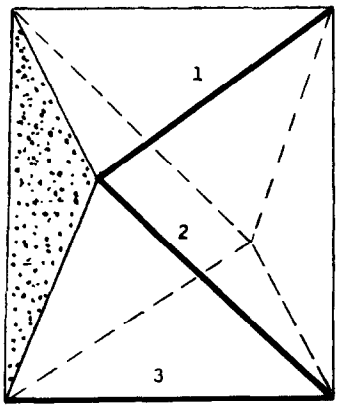

FIG. 5. The terminal Ti_1 and Ti_2 octahedra both share a face and three edges as shown above, but Ti_1 shares edge 1 with the chain segment it terminates while Ti_2 shares edge 3.

too surprising that Ti_4O_7 (and to a lesser extent Ti_5O_9) turns out to be different from the others. The two chain segments differ in the distribution of valence along them, both in the shear-plane region and in the rutile-like region. In addition, although their geometrical relation to the neighboring chains is similar at first glance, the two chain segments differ in the terminal octahedra which share both one face and three edges in the same relative position, but the edge shared with the segment it terminates differs for Ti_1 and Ti_2 as shown in Fig. 5.

Distortions of the Ti–O Distances

The standard deviations of the Ti–O distances can be used as a measure of the distortion of the TiO_6 octahedra (Table V). This analysis supports the decomposition in two regions, the shear-plane region being

TABLE III

BOND DISTANCES (Å) IN THE SERIES

Ti_4O_7	Ti_5O_9	Ti_6O_{11}	Ti_7O_{13}	Ti_8O_{15}	Ti_9O_{17}
					Ti(1,0)
					O(1,0) 1.991
					O(1,0) 1.991
					O(3,0) 1.972
					O(3,1) 1.966
					O(3,0) 1.972
					O(3,1) 1.966
			Ti(1,0)	Ti(1,1)	Ti(1,1)
			O(1,0) 1.991	O(1,1) 1.995	O(1,1) 1.993
			O(1,0) 1.991	O(2,0) 1.981	O(2,0) 1.983
			O(3,0) 2.005	O(3,1) 1.958	O(3,1) 1.957
			O(3,1) 2.018	O(3,2) 2.024	O(3,2) 2.024
			O(3,0) 2.005	O(3,1) 1.952	O(3,0) 1.943
			O(3,1) 2.018	O(4,0) 2.004	O(4,0) 1.989
	Ti(1,0)	Ti(1,1)	Ti(1,1)	Ti(1,2)	Ti(1,2)
	O(1,0) 1.974	O(1,1) 1.983	O(1,1) 1.987	O(1,2) 1.974	O(1,2) 1.979
	O(1,0) 1.974	O(2,0) 1.976	O(2,0) 1.971	O(2,1) 1.980	O(2,1) 1.978
	O(3,0) 2.008	O(3,1) 1.967	O(3,1) 1.932	O(3,2) 1.931	O(3,2) 1.938
	O(3,1) 2.008	O(3,2) 2.040	O(3,2) 2.035	O(3,3) 2.043	O(3,3) 2.040
	O(3,0) 2.008	O(3,1) 1.973	O(3,0) 1.902	O(4,0) 1.893	O(4,0) 1.895
	O(3,1) 2.008	O(4,0) 2.029	O(4,0) 2.018	O(4,0) 2.002	O(4,1) 1.994
Ti(1,1)	Ti(1,1)	Ti(1,2)	Ti(1,2)	Ti(1,3)	Ti(1,3)
O(1,1) 2.064	O(1,1) 2.094	O(1,2) 2.113	O(1,2) 2.107	O(1,3) 2.113	O(1,3) 2.112
O(2,0) 1.930	O(2,0) 1.906	O(2,1) 1.884	O(2,1) 1.880	O(2,2) 1.869	O(2,2) 1.873
O(3,1) 2.011	O(3,1) 1.987	O(3,2) 1.973	O(3,2) 1.977	O(3,3) 1.982	O(3,3) 1.985
O(3,2) 2.060	O(3,2) 2.093	O(3,3) 2.100	O(3,3) 2.100	O(3,4) 2.097	O(3,4) 2.098
O(3,1) 1.976	O(3,0) 1.944	O(4,0) 1.881	O(4,0) 1.870	O(4,1) 1.876	O(4,1) 1.876
O(4,0) 1.997	O(4,0) 1.995	O(4,1) 1.967	O(4,1) 1.957	O(4,2) 1.950	O(4,2) 1.950
Ti(1,2)	Ti(1,2)	Ti(1,3)	Ti(1,3)	Ti(1,4)	Ti(1,4)
O(3,2) 1.996	O(3,2) 1.979	O(3,3) 1.971	O(3,3) 1.968	O(3,4) 1.970	O(3,4) 1.969
O(2,1) 2.001	O(2,1) 2.004	O(2,2) 2.000	O(2,2) 1.994	O(2,3) 1.987	O(2,3) 1.993
O(3,2) 2.177	O(3,2) 2.186	O(3,3) 2.199	O(3,3) 2.207	O(3,4) 2.211	O(3,4) 2.207
O(1,1) 2.118	O(1,1) 2.134	O(1,2) 2.118	O(1,2) 2.118	O(1,3) 2.116	O(1,3) 2.119
O(4,0) 1.939	O(4,0) 1.884	O(4,1) 1.884	O(4,1) 1.886	O(4,2) 1.887	O(4,2) 1.886
O(4,1) 1.877	O(4,1) 1.856	O(4,2) 1.842	O(4,2) 1.840	O(4,3) 1.827	O(4,3) 1.832

TABLE III—*Continued*

Ti_4O_7	Ti_5O_9	Ti_6O_{11}	Ti_7O_{13}	Ti_8O_{15}	Ti_9O_{17}
	---------- Shear plane ----------				
Ti(2,2)	Ti(2,2)	Ti(2,3)	Ti(2,3)	Ti(2,4)	Ti(2,4)
O(1,1) 2.064	O(1,1) 2.053	O(1,2) 2.046	O(1,2) 2.048	O(1,3) 2.040	O(1,3) 2.042
O(3,2) 2.022	O(3,2) 2.040	O(3,3) 2.059	O(3,3) 2.068	O(3,4) 2.066	O(3,4) 2.072
O(2,1) 1.994	O(2,1) 1.993	O(2,2) 1.993	O(2,2) 1.988	O(2,3) 1.999	O(2,3) 1.998
O(3,1) 1.856	O(3,1) 1.842	O(3,2) 1.847	O(3,2) 1.854	O(3,3) 1.847	O(3,3) 1.848
O(4,1) 1.935	O(4,1) 1.943	O(4,2) 1.961	O(4,2) 1.959	O(4,3) 1.971	O(4,3) 1.968
O(2,1) 2.156	O(2,1) 2.155	O(2,2) 2.149	O(2,2) 2.144	O(2,3) 2.143	O(2,3) 2.145
Ti(2,1)	Ti(2,1)	Ti(2,2)	Ti(2,2)	Ti(2,3)	Ti(2,3)
O(2,0) 1.940	O(1,0) 1.930	O(1,1) 1.941	O(1,1) 1.944	O(1,2) 1.958	O(1,2) 1.959
O(1,1) 2.041	O(1,1) 2.036	O(1,2) 2.032	O(1,2) 2.030	O(1,3) 2.037	O(1,3) 2.041
O(2,0) 1.977	O(2,0) 1.976	O(2,1) 1.994	O(2,1) 1.996	O(2,2) 2.005	O(2,2) 2.006
O(2,1) 2.069	O(2,1) 2.071	O(2,2) 2.065	O(2,2) 2.067	O(2,3) 2.062	O(2,3) 2.061
O(4,0) 1.935	O(3,0) 1.906	O(3,1) 1.901	O(3,1) 1.907	O(3,2) 1.912	O(3,2) 1.913
O(4,1) 2.070	O(4,1) 2.085	O(3,2) 2.077	O(4,2) 2.079	O(4,3) 2.083	O(4,3) 2.079
	Ti(2,0)	Ti(2,1)	Ti(2,1)	Ti(2,2)	Ti(2,2)
	O(2,0) 1.970	O(2,0) 1.944	O(1,0) 1.943	O(1,1) 1.935	O(1,1) 1.941
	O(1,0) 1.955	O(1,1) 1.951	O(1,1) 1.957	O(1,2) 1.951	O(1,2) 1.951
	O(1,0) 1.955	O(2,0) 1.953	O(2,0) 1.946	O(2,1) 1.948	O(2,1) 1.948
	O(2,0) 1.970	O(2,1) 1.979	O(2,1) 1.983	O(2,2) 1.980	O(2,2) 1.979
	O(4,0) 2.015	O(4,0) 1.966	O(3,0) 1.937	O(3,1) 1.936	O(3,1) 1.935
	O(4,0) 2.015	O(4,1) 2.051	O(4,1) 2.060	O(4,2) 2.067	O(4,2) 2.070
			Ti(2,0)	Ti(2,1)	Ti(2,1)
			O(2,0) 1.957	O(1,1) 1.963	O(1,0) 1.953
			O(1,0) 1.948	O(2,0) 1.940	O(1,1) 1.964
			O(1,0) 1.948	O(2,0) 1.961	O(2,0) 1.943
			O(2,0) 1.957	O(2,1) 1.949	O(2,1) 1.957
			O(4,0) 2.003	O(4,0) 1.967	O(3,0) 1.956
			O(4,0) 2.003	O(4,1) 2.019	O(4,1) 2.032
					Ti(2,0)
					O(2,0) 1.956
					O(1,0) 1.954
					O(1,0) 1.954
					O(2,0) 1.956
					O(4,0) 1.987
					O(4,0) 1.987

Note. The oxygen neighbors around each Ti in a given chain segment are mentioned in the same order so that distortions in a given chain segment can be compared vertically while distortions for different members can be compared horizontally. The sigmas on Ti–O distances are 0.001 for $n = 4$ and 5, 0.003 for $n = 6$ and 7, and 0.002 for $n = 8$ and 9.

more distorted than the rutile-like region. Two features are remarkably consistent throughout the series: the constancy of the distortion in the shear-plane region and the differences in distortion between chains 1 and 2. This supports the above description of the geometry of the slabs as fixed.

Ti–Ti Distances

Like the distortions of the Ti–O dis-

TABLE IV

IONIC VALENCES OF THE Ti ATOMS FOR THE SERIES AT ROOM TEMPERATURE (THE ORDER IS THE SAME AS IN TABLE III

Ti_4O_7	Ti_5O_9	Ti_6O_{11}	Ti_7O_{13}	Ti_8O_{15}	Ti_9O_{17}
					3.88
			3.53	3.76	3.82
	3.63	3.66	3.90	3.95	3.95
3.51	3.55	3.76	3.81	3.82	3.81
3.37	3.50	3.56	3.56	3.59	3.58
----------	Shear plane	----------			
3.54	3.54	3.48	3.47	3.46	3.44
3.53	3.58	3.57	3.54	3.47	3.47
	3.83	3.91	3.94	3.96	3.95
			3.96	4.00	3.97
					4.00

TABLE V

STANDARD DEVIATIONS OF THE OBSERVED Ti–O DISTANCES AS A MEASURE OF THE DISTORTION AROUND Ti ATOMS

Ti_4O_7	Ti_5O_9	Ti_6O_{11}	Ti_7O_{13}	Ti_8O_{15}	Ti_9O_{17}
					0.011
			0.011	0.025	0.026
	0.016	0.029	0.046	0.048	0.045
0.047	0.070	0.092	0.094	0.096	0.095
0.102	0.120	0.124	0.127	0.130	0.129
----------	Shear plane	----------			
0.095	0.097	0.093	0.092	0.091	0.092
0.057	0.068	0.064	0.062	0.059	0.058
	0.026	0.036	0.043	0.046	0.043
			0.024	0.025	0.030
					0.015

tances discussed above, the pattern of the Ti–Ti distances shows remarkable similarities between corresponding atoms for different values of n and consistent differences between the patterns of the two chain segments. The Ti–Ti distances along the chains are listed in Table VI. As expected, the shortest distances (2.81 to 2.83 Å) are found between octahedra sharing a face across the shear plane. In chain 1 and for all values of n, the Ti atoms in the shear-plane region are farthest apart (3.02 to 3.05 Å), whereas such distances gradually decrease toward the center of the rutile segments. In

TABLE VI

Ti–Ti DISTANCES IN THE [$\bar{1}$01] CHAINS AND IN THE [010] CHAINS

	Ti_4O_7	Ti_5O_9	Ti_6O_{11}	Ti_7O_{13}	Ti_8O_{15}	Ti_9O_{17}	
					2.910	2.939	
			2.876	2.901	2.927	2.935	
	2.941	2.925	2.966	2.985	2.989	2.986	
	3.019	3.042	3.053	3.054	3.047	3.048	
	2.812	2.829	2.833	2.828	2.831	2.830	Shear plane
	3.020	3.005	2.973	2.961	2.946	2.948	
	2.894	2.929	2.958	2.970	2.975	2.975	
			2.938	2.947	2.953	2.960	
					2.957	2.962	
Terminal Ti in the segment (See Fig. 4)							
Ti_1–Ti_1	3.280	3.274	3.278	3.281	3.278	3.276	
Ti_1–Ti_2	2.812	2.829	2.833	2.828	2.831	2.830	
Ti_2–Ti_2	3.237	3.256	3.263	3.259	3.263	3.261	

Note. For odd n the order is the same as in the previous tables, for even n the first distance mentioned is the Ti(1,1)–Ti(1,1) bond through the center of symmetry at the origin.

contrast, such distances are almost constant along chain 2 for $n = 6$ to 9 with distances ranging from 2.94 to 2.97 Å. However, Ti_4O_7 and Ti_5O_9 differ markedly from the rest of the series in this respect.

The Ti–Ti distances in the **b** chain are virtually constant throughout the series.

No comparison with the homologous series V_nO_{2n-1} (*12*) was attempted because the present contribution deals with Ti only.

Conclusions

The analysis of the cells (*9*) and structures of the Ti_nO_{2n-1}, $4 \leq n \leq 9$, series at room temperature confirms the considerable similarity of these compounds that could be expected from their common building principle. No even–odd alternance was disclosed by the analysis, even for the ionic valences, but Ti_4O_7 shows some slight departures from an otherwise remarkably homogeneous family. This individual behavior is attributed to the absence of a rutile-like slab in between the shear-region slabs.

References

1. S. Andersson, B. Collen, U. Kuylenstierna, and A. Magnéli, *Acta Chem. Scand.* **11**, 1641 (1957).
2. S. Andersson and L. Jahnberg, *Ark. Kemi* **21**, 413 (1961).
3. L. A. Bursill and B. G. Hyde, *Prog. Solid State Chem.* **7**, 177 (1972).
4. R. F. Bartholomew and W. B. White, *J. Cryst. Growth* **6**, 249 (1970).
5. M. Marezio, D. B. McWhan, P. D. Dernier, and J. P. Remeika, *J. Solid State Chem.* **6**, 213 (1973).
6. M. Marezio, D. Tranqui, S. Lakkis, and C. Schlenker, *Phys. Rev. B* **16**, 2811 (1977).
7. P. Strobel and Y. Le Page, *J. Cryst. Growth* **56**, 723 (1982).
8. P. Strobel and Y. Le Page, *J. Mater. Sci.* **17** (1982), in press.
9. Y. Le Page and P. Strobel, *J. Solid State Chem.*, (1982), in press.
10. A. C. Larson, *in* "Crystallographic Computing," (F. R. Ahmed, Ed.), pp. 291–294, Munksgaard, Copenhagen (1970).
11. D. T. Cromer and J. T. Waber, *in* "International Tables for X-Ray Crystallography," Vol. IV, p. 99, Kynoch Press, Birmingham (1974).
12. H. Horiuchi, N. Morimoto, and M. Tokonami, *J. Solid State Chem.* **17**, 407 (1976).